



Synthesis of polyaspartic acid/2-amino-2-methyl-1,3-propanediol graft copolymer and evaluation of its scale inhibition and corrosion inhibition performance

Ben Zhang, Juan Li, Xiaogai Lv, Yuanchen Cui, Ying Xu*

College of Chemistry and Chemical Engineering, Henan University, Kaifeng 475004, China, Tel. +86 378 3881358; email: hdccxu@126.com

Received 15 August 2013; Accepted 27 January 2014

ABSTRACT

Polyaspartic acid/2-amino-2-methyl-1,3-propanediol graft copolymer, a novel non-phosphorus scale and corrosion inhibitor, was synthesized and characterized by infrared spectroscopy. Its performance was evaluated by static scale inhibition method and dynamic corrosion testing. It was found that the graft copolymer showed excellent inhibition ability against CaCO_3 , CaSO_4 , and $\text{Ca}_3(\text{PO}_4)_2$ scales and a definite inhibition corrosion performance as well. The inhibition efficiency was close to 99.9% against CaCO_3 , CaSO_4 , and $\text{Ca}_3(\text{PO}_4)_2$ when the inhibitor was at an appropriate concentration. The inhibitor had still possessed higher antiscaling efficiency against CaCO_3 with increasing concentration of Ca^{2+} and heating time. In addition, The graft copolymer could change the structure of crystals CaCO_3 , CaSO_4 , and $\text{Ca}_3(\text{PO}_4)_2$ by observation of scanning electron microscopy.

Keywords: Polyaspartic acid/2-amino-2-methyl-1,3-propanediol; Scale inhibition; Corrosion inhibition

1. Introduction

Natural water used in the water processing industry contains ions i.e. Ca^{2+} , Mg^{2+} , HCO_3^- , SO_4^{2-} , and PO_4^{3-} [1]. The precipitation of mineral scales containing CaCO_3 , CaSO_4 , and $\text{Ca}_3(\text{PO}_4)_2$ on heat transfer surfaces widely occurs, which caused many problems such as corrosion of pipeline and decrease of thermal efficiency [2]. To lengthen service life of equipment and improve reuse efficiency of water, chemical inhibitors are usually used in industrial circulating cool water [3–6]. In recent years, with increasing environmental concerns and discharge limitations, the concept of “green chemistry” was proposed, and green scale

inhibitors have become an important focus in water treatment technology [7–9]. Polyaspartic acid (PASP), a phosphate-free, non-toxic, biodegradable polymer, is the representative of the environmental friendly water treatment agents [10–12]. Although PASP possesses excellent inhibition performance against CaCO_3 and CaSO_4 scales, it has poor ability against $\text{Ca}_3(\text{PO}_4)_2$ scale and is not applied to high-hardness water [13]. Polysuccinimide (PSI), intermediate of PASP, is easily obtained open-loop by amino to generate the PASP derivatives containing side chain of the functional groups [14], as shown in Fig. 1. These derivatives can have good comprehensive performance.

In this paper, 2-amino-2-methyl-1,3-propanediol, double hydroxyl compound, was used to modify

*Corresponding author.

PASP. The PASP/2-amino-2-methyl-1,3-propanediol graft copolymer was obtained and characterized by infrared spectroscopy (IR). Its performance of scale inhibition and corrosion inhibition was measured by static and dynamic tests. The CaCO_3 , CaSO_4 , and $\text{Ca}_3(\text{PO}_4)_2$ scales were observed by scanning electron microscopy (SEM).

2. Experimental

2.1. Reagents and instruments

2-Amino-2-methyl-1,3-propanediol was purchased from Aladdin Chemical Reagent Co. Ltd (Shanghai, P.R. China). Ethylenediaminetetraacetic acid disodium salt and Eriochrome black T were obtained from Tianjin Chemical Reagent Factory (Tianjin, P.R. China). Maleic anhydride, urea, ascorbic acid, and antimony potassium tartrate were obtained from Sinopharm Chemical Reagent Co. Ltd (Shanghai, P.R. China). Ammonium molybdate tetrahydrate was supplied from Kemiou Chemical Reagent Co. Ltd (Tianjin, P.R. China). All the chemicals in this study are of analytical reagent grade.

AVATAR-360 Fourier transform infrared spectroscopy (FT-IR), JSM5600LV SEM, RCC-III rotation coupon corrosion tester instruments, the model TG16-WS centrifuges, and 723N grating spectrophotometer are used in the present research.

2.2. Synthesis of polyaspartic acid/2-amino-2-methyl-1,3-propanediol graft copolymer

PSI was first synthesized in the present work [15]. The aqueous solution of 2-amino-2-methyl-1,3-propanediol (approximately 0.05 g/mL) was added slowly to the suspension liquid of PSI (approximately 0.06 g/mL), the molar ratio of both was 1:1, and reacted for 24 h at 60°C until the mixture became transparent. The total volume of the aqueous solution was about 30 mL after the reaction was complete. The pH value of the mixture was adjusted to 7.0 with HCl solution. Then, the salt solution was added to ethanol dropwise by charging hopper with stirring at a volume ratio of 1:5

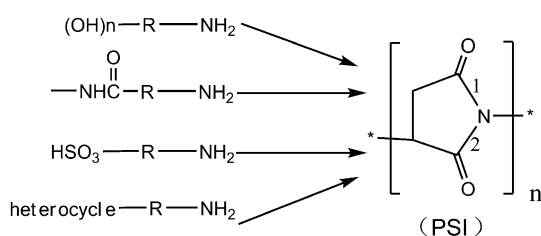


Fig. 1. Modification route of PASP.

and centrifuged. The target compound, reddish-brown PASP/2-amino-2-methyl-1,3-propanediol graft copolymer was obtained. Relevant synthetic reaction is expressed in Fig. 2.

3. Results and discussion

3.1. FT-IR analysis of synthetic products

The FT-IR spectra of PSAP (a) and PASP/2-amino-2-methyl-1,3-propanediol graft copolymer (b) are shown in Fig. 3. It is seen from curve (a) that 1,599 cm^{-1} is asymmetric stretch absorption peak of the carboxyl anion, which is the characteristic absorption peak of amino acid; and 1,399 cm^{-1} is symmetric stretching peak of the carboxyl anion, indicating that it is PASP. In curve (b), 1,062 cm^{-1} is the characteristic absorption peaks of the C–O bonds, indicating that it is PASP/2-amino-2-methyl-1,3-propanediol graft copolymer [16,17].

3.2. The performance evaluation

3.2.1. The inhibition efficiency of graft copolymer against CaCO_3 scale

The inhibition efficiency of the graft copolymer against CaCO_3 scale was calculated according to Eq. (1). The concentration of Ca^{2+} and HCO_3^- is 250 mg/L, the heating time is 6 h, and the temperature is 80°C (Langelier saturation index, LSI=1.74). Fig. 4 shows the variation of inhibition efficiency against CaCO_3 scale with different concentrations of the graft copolymer. As seen in Fig. 4, PASP/2-amino-2-methyl-1,3-propanediol shows excellent inhibitory performance and the inhibition efficiency is increases with its concentration increase. When the dosage is above 1 mg/L, the inhibition efficiency is close to 100% and the graft copolymer availably controls the deposition of scale.

$$\eta_{\text{CaCO}_3} = \frac{V_1 - V_0}{V_2 - V_0} \times 100\% \quad (1)$$

where V_0 is the volume of EDTA in the absence of scale inhibitor after incubation for 6 h, V_1 is the volume of EDTA in the presence of scale inhibitor after incubation for 6 h, and V_2 is the mass volume of EDTA all in to-be-tested solution.

3.2.2. The effect of graft copolymer on the concentration Ca^{2+}

We expanded the range of experimental conditions of CaCO_3 scale because it is the major component of

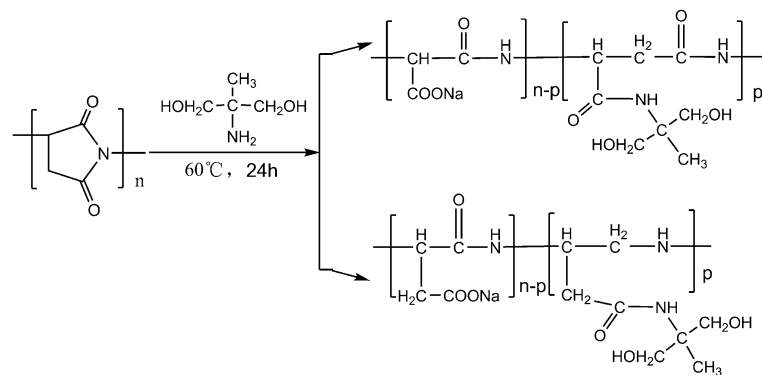


Fig. 2. Synthesis route of PASP/2-amino-2-methyl-1,3-propanediol graft copolymer.

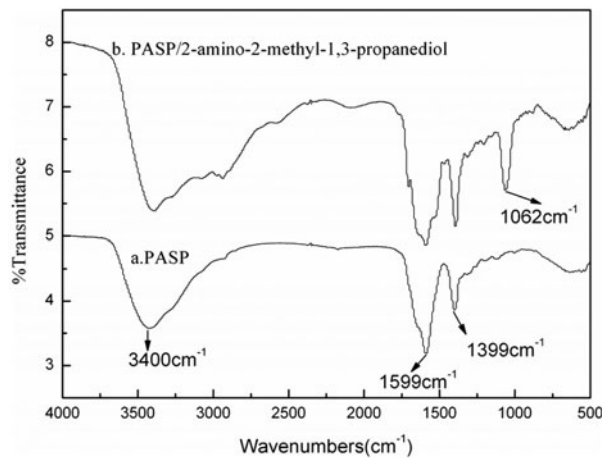


Fig. 3. IR of PASP and PASP/2-amino-2-methyl-1,3-propanediol graft copolymer.

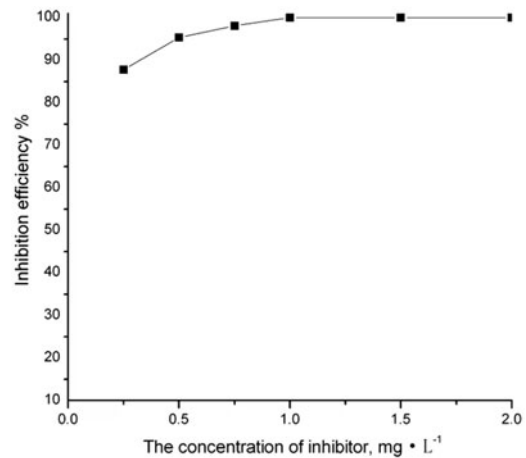


Fig. 4. The inhibition efficiency of PASP/2-amino-2-methyl-1,3-propanediol against CaCO_3 .

scale. The concentration of Ca^{2+} and HCO_3^- is at a range of 250–500 mg/L, the heating time is 6 h, the temperature is 80°C, and the concentration of medication is 1 mg/L. Fig. 5 shows that the influence of the concentration of Ca^{2+} on the inhibition efficiency of the grafted copolymer. The PASP/2-amino-2-methyl-1,3-propanediol still has outstanding performance against CaCO_3 scale in high-hardness water. When concentration of Ca^{2+} and HCO_3^- is 500 mg/L, the inhibition efficiency remains 89.5%. This is due to the impact of the presence of double hydroxyl in PASP/2-amino-2-methyl-1,3-propanediol side chain.

3.2.3. The Influence of heating time on graft copolymer inhibition efficiency

Fig. 6 presents the relationship between the inhibition efficiency of PASP/2-amino-2-methyl-1,3-propanediol graft copolymer and the heating time. The

heating time is at a range of 3–16 h, the concentration of Ca^{2+} and HCO_3^- is 250 mg/L, the temperature is 80°C, and the concentration of graft copolymer is 1 mg/L. The inhibition efficiency was still close to 100% when the heating time lengthened to 16 h. It indicated that the stability and chelating ability of scale inhibitor were very good.

3.2.4. The inhibition efficiency of graft copolymer against CaSO_4 scale

The inhibition efficiency of the scale inhibition against CaSO_4 scale was calculated according to Eq. (1). The concentration of Ca^{2+} and SO_4^{2-} is 7,100 and 6,800 mg/L separately, the heating time is 6 h, and the temperature is 70°C (saturation index, $\text{SI} = 0.53$). Fig. 7 shows the relationship between the inhibition efficiency and the concentration of graft copolymer. It can be found that PASP/2-amino-2-methyl-1,3-propanediol

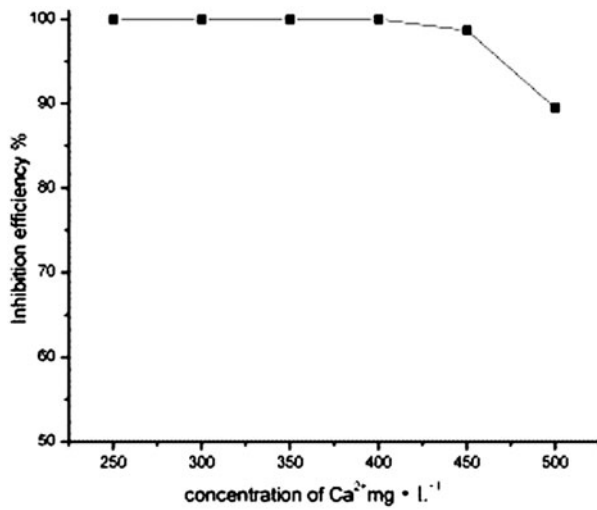


Fig. 5. The effect of PASP/2-amino-2-methyl-1,3-propanediol on the concentration Ca²⁺.

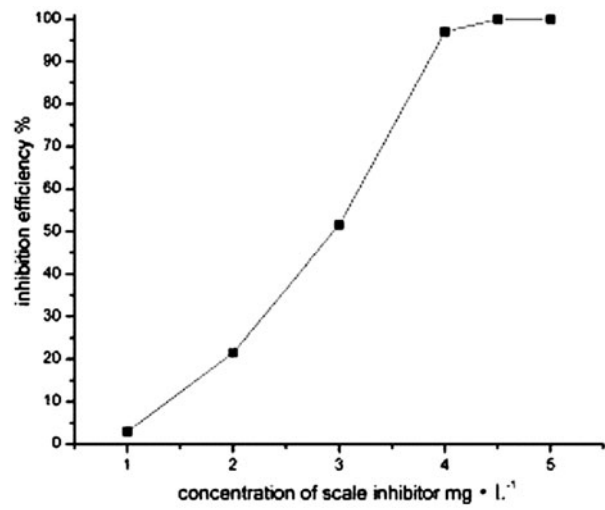


Fig. 7. The inhibition efficiency of PASP/2-amino-2-methyl-1,3-propanediol against CaSO₄.

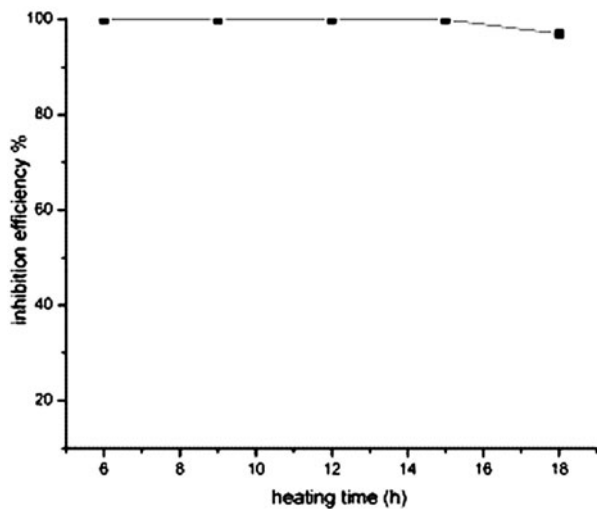


Fig. 6. Influence of the heating time on PASP/2-amino-2-methyl-1,3-propanediol

has a superior inhibition ability for CaSO₄ scale. When its concentration was 4.5 mg/L, the inhibition efficiency was close 100%.

3.2.5. The inhibition efficiency of graft copolymer against Ca₃(PO₄)₂ scale

The inhibition efficiency of the grafted copolymer against Ca₃(PO₄)₂ scale was determined by the ascorbic acid–phosphomolybdic blue method and calculated according to Eq. (2). The concentration of Ca²⁺ and PO₄³⁻ is 250 and 10 mg/L separately, the heating

time is 10 h, and the temperature is 80 °C (SI = 0.4). It is reported that the inhibition efficiency of PASP against Ca₃(PO₄)₂ scale was only about 20% when its concentration was at a range of 10–20 mg/L [18,19]. The introduction of hydroxyl can't improve efficiency of PASP against CaCO₃, but it can greatly improve the efficiency against Ca₃(PO₄)₂ [20,21]. Fig. 8 shows the inhibition efficiency of the graft copolymer against Ca₃(PO₄)₂ scale. It can be seen that the inhibition efficiency reached 40% when the antiscalant concentration was 8 mg/L. With dosage rising, the scale inhibition efficiency increases. When scale inhibitor was 16 mg/L, it achieved 97.5%. This result may relate to the double hydroxyl of 2-amino-2-methyl-1,3-propanediol.

$$\eta_{Ca_3(PO_4)_2} = \frac{\rho_1 - \rho_0}{\rho_2 - \rho_0} \times 100\% \quad (2)$$

where ρ_0 is the concentration of PO₄³⁻ in the absence of scale inhibitor in to-be-tested solution; ρ_1 is the concentration of PO₄³⁻ in the presence of scale inhibitor in to-be-tested solution; and ρ_2 is the mass concentration of all in to-be-tested solution.

3.2.6. Inhibition corrosion efficiency of grafted copolymer

The corrosion inhibition efficiency of PASP/2-amino-2-methyl-1,3-propanediol was measured by weight loss of rotating hung steel slices [22]. The 20# carbon steel (50 × 25 × 2 mm) was used in the simulation experiment and its chemical composition is listed in Table 1; 1.11 g of CaCl₂, 0.986 g of MgSO₄·7H₂O,

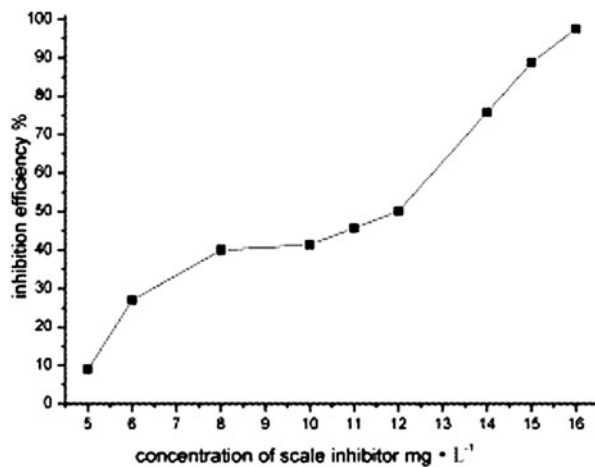


Fig. 8. The inhibition efficiency of PASP/2-amino-2-methyl-1,3-propanediol against $\text{Ca}_3(\text{PO}_4)_2$.

0.336 g of NaCl, and 0.336 g of NaOH were added into a beaker of 2 L and a simulated solution prepared. The temperature, rotating speed of system, and the reaction time were $45 \pm 1^\circ\text{C}$, 75 ± 1 RPM, and 72 h, respectively [23]. The corrosion inhibition efficiency was calculated according to Eqs. (3) and (4).

$$v = \frac{87600 \times [(m_0 - m_1) - \Delta m]}{S \times T \times D} \quad (3)$$

$$\eta = \frac{v_0 - v}{v_0} \times 100\% \quad (4)$$

where m_0 is the mass of carbon steel hung slices before test; m_1 is the mass of carbon steel hung slices after test; Δm is the mass loss of carbon steel hung slices caused by washing in acid (5% HCl and 3 g/L of hexamethylene tetramine). S is the surface area of carbon steel hung slice (28 cm^2). T is testing time (72 h). D is density of carbon steel hung slices (7.85 g/cm^3), v_0 is annual corrosion rate in the absence of scale inhibitor (mm/y), v is annual corrosion efficiency in the presence of scale inhibitor (mm/y), η is corrosion inhibition efficiency (%).

The Inhibition corrosion efficiency of PASP/2-amino-2-methyl-1,3-propanediol is shown in Fig. 9.

We can see that the corrosion inhibition efficiency of graft copolymer is not highlighted. It reached 18.3% when the inhibitor concentration was 12 mg/L. It might be because the micromolecule, 2-amino-2-methyl-1,3-propanediol, has corrosion effect on copper, aluminum, and other metals. Therefore, when the micromolecule was grafted onto the side chain of PASP, the inhibition corrosion result was not obvious.

3.2.7. The effect of grafted copolymer on the morphologies of CaCO_3 , $\text{Ca}_3(\text{PO}_4)_2$, and CaSO_4 crystals

As shown in Fig. 10(a), CaCO_3 crystal obtained without inhibitor was of a well-defined rhombohedral characteristic corresponding to calcite phase. Nevertheless, when the inhibitor was added to solution, the regular shape disappeared and the CaCO_3 crystal (Fig. 10(b)) became vaterite [24]. The precipitation of $\text{Ca}_3(\text{PO}_4)_2$ (Fig. 10(c) and (d)) was similar to CaCO_3 precipitation, the crystal became distorted because of the addition of graft copolymer. CaSO_4 crystal (Fig. 10(e)) in the absence of inhibitor was regular rod shaped, the crystal morphology changed into fish-bone-like structure (Fig. 10(f)) with the addition of

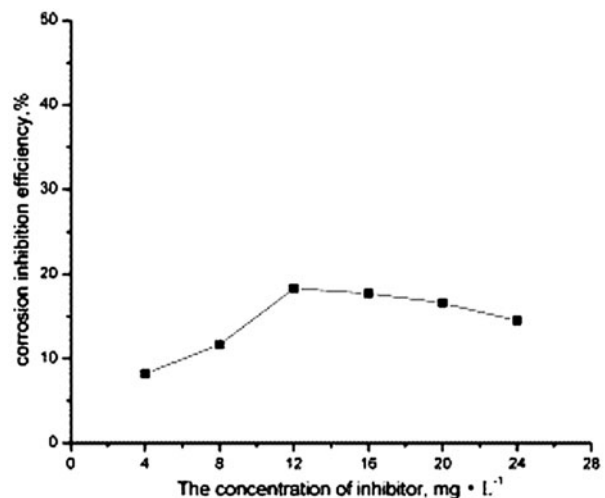


Fig. 9. Inhibition corrosion efficiency of PASP/2-amino-2-methyl-1,3-propanediol.

Table 1
Chemical composition of 20[#] carbon steel

Elements	C	Si	Mn	P	S	Cr	Ni	Cu	Fe
Weight (%)	0.17–0.23	0.17–0.37	0.35–0.65	≤0.035	≤0.035	≤0.25	≤0.3	≤0.25	≥98.32

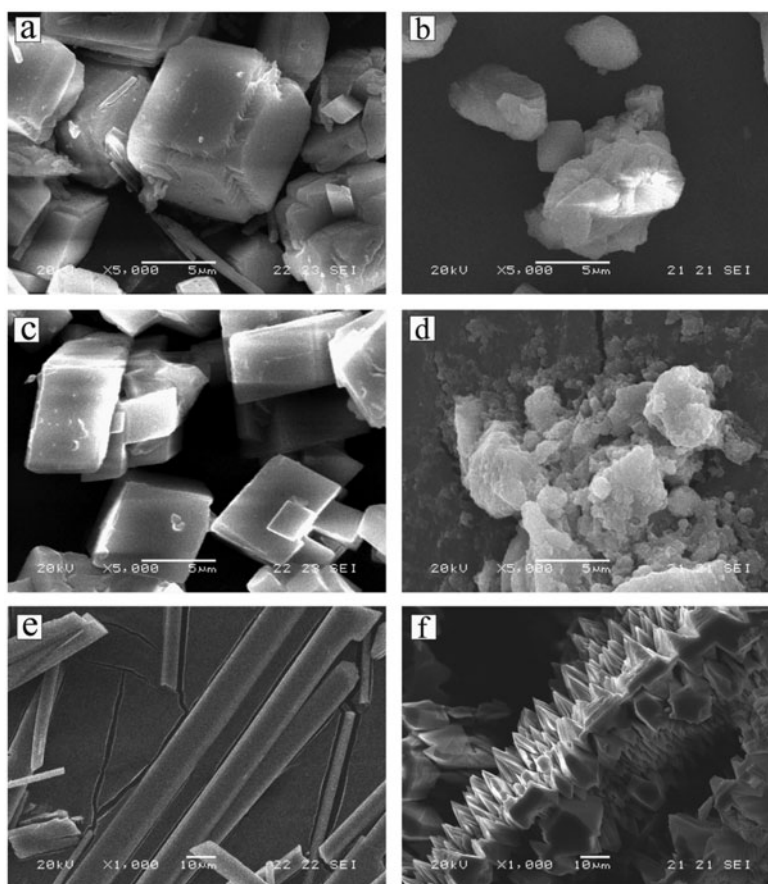


Fig. 10. SEM images of CaCO_3 , $\text{Ca}_3(\text{PO}_4)_2$, and CaSO_4 crystals, (a), (c), and (e) in the absence of inhibitor and (b), (d), and (f) in the presence of grafted copolymer.

PASP/2-amino-2-methyl-1,3-propanediol. As you can see in the above SEM figures, the PASP/2-amino-2-methyl-1,3-propanediol is adsorbed onto the active sites of the crystal nucleus, which disrupts the growth habit and crystallization process of the crystals. The precipitates could not cover equipment surfaces.

4. Conclusions

PASP/2-amino-2-methyl-1,3-propanediol graft copolymer was synthesized. Its scale and corrosion inhibition performance were evaluated by static scale inhibition method and dynamic corrosion testing. The results indicated that the inhibition efficiency was close to 99.9% against CaCO_3 , CaSO_4 , and $\text{Ca}_3(\text{PO}_4)_2$ when the concentration of inhibitor was 1, 4.5, and 16 mg/L, respectively. Meanwhile, the graft copolymer still possessed excellent inhibition ability for CaCO_3 scale when experimental conditions were expanded. And the graft copolymer owned a certain corrosion inhibition capability. The corrosion inhibition efficiency could reach 18.3%, when its concentration was

12 mg/L. In addition, PASP/2-amino-2-methyl-1,3-propanediol disrupts the growth habit and crystallization process of the crystals.

Acknowledgment

This work was supported by the Fund of Henan Province Science & Technology (122102310348).

References

- [1] K. Chauhan, R. Kumar, M. Kumar, Modified pectin-based polymers as green antiscalants for calcium sulfate scale inhibition, *Desalination* 305 (2012) 31–37.
- [2] C. Wang, S.P. Li, T.D. Li, Calcium carbonate inhibition by a phosphonate-terminated poly(maleic-co-sulfonate) polymeric inhibitor, *Desalination* 249 (2009) 1–4.
- [3] X.H. Qiang, Z.H. Sheng, H. Zhang, Study on scale inhibition performances and interaction mechanism of modified collagen, *Desalination* 309 (2013) 237–242.
- [4] R. Touir, N. Dkhireche, M. Ebn Touhami, Study of phosphonate addition and hydrodynamic conditions on ordinary steel corrosion inhibition in simulated cooling water, *Mater. Chem. Phys.* 122 (2010) 1–9.

- [5] X.X. Xue, C.G. Fu, N. Li, F.F. Zheng, W.B. Yang, X.D. Yang, Performance of a non-phosphorus antiscalant on inhibition of calcium-sulfate precipitation, *Water Sci. Technol.* 66 (2012) 193–200.
- [6] D. Hasson, H. Shemer, A. Sher, State of the art of friendly “green” scale control inhibitors: A review article, *Ind. Eng. Chem. Res.* 50 (2011) 7601–7607.
- [7] D. Liu, W.B. Dong, F.T. Li, F. Hui, J. Lédion, Comparative performance of polyepoxysuccinic acid and polyaspartic acid on scaling inhibition by static and rapid controlled precipitation methods, *Desalination* 304 (2012) 1–10.
- [8] A. Martinod, M. Euvrard, A. Foissy, A. Neville, Progressing the understanding of chemical inhibition of mineral scale by green inhibitors, *Desalination* 220 (2008) 345–352.
- [9] Y. Xu, L.N. Wang, L.L. Zhao, Y.C. Cui, Synthesis of polyaspartic acid–aminobenzenesulfonic acid grafted copolymer and its scale inhibition performance and dispersion capacity, *Water Sci. Technol.* 64 (2011) 423–430.
- [10] A. Martinod, A. Neville, M. Euvrad, Electrodeposition of a calcareous layer: Effects of green inhibitors, *Chem. Eng. Sci.* 64 (2009) 2413–2421.
- [11] Z.Y. Liu, Y.H. Sun, X.H. Zhou, T. Wu, Y. Tian, Y.Z. Wang, Synthesis and scale inhibitor performance of polyaspartic acid, *J. Environ. Sci.* 23 (2011) S153–S155.
- [12] L.E. Nita, A.P. Chiriac, C.M. Popescu, I. Neamtu, L. Alecu, Possibilities for poly(aspartic acid) preparation as biodegradable compound, *J. Optoelectron. Adv. Mater.* 8 (2006) 663–666.
- [13] J.S. Tang, S.L. Fu, D.H. Emmons, Biodegradable modified polyaspartic polymers for corrosion and scale control [P], 2000, US 6022401.
- [14] T. Nakato, M. Tomida, M. Suwa, Y. Morishima, A. Kusuno, T. Kakuchi, Preparation and characterization of dodecylamine-modified poly(aspartic acid) as a biodegradable water-soluble polymeric material, *Polym. Bull.* 44 (2000) 385–391.
- [15] Y. Xu, B. Zhang, L.L. Zhao, Y.C. Cui, Synthesis of polyaspartic acid/5-aminoorotic acid graft copolymer and evaluation of its scale inhibition and corrosion inhibition performance, *Desalination* 311 (2013) 156–161.
- [16] R.M. Silverstein, F.X. Webster, D.J. Kiemle, *Spectrometric Identification of Organic Compounds*, East China University of Science and Technology Publications, Shanghai, 2007, pp. 100, 105.
- [17] Y.S. Zhao, G.W. Yuan, Y.M. Liu, X.J. Ma, M.J. Guo, K. Chen, Study on scale inhibition performance of polyaspartic acid derivatives with di-hydroxyl group on $\text{Ca}_3(\text{PO}_4)_2$, *Environ. Chem.* 28 (2009) 506–509.
- [18] M.F. Yan, Z.F. Liu, L.H. Zhang, Y.H. Gao, Y.J. Wu, Y.M. Chen, Synthesis and performance research of polyaspartic acid graft copolymers, *J. Hebei Acad. Sci.* 23 (2006) 67–69.
- [19] Z.Q. Liang, J.N. Li, X. Zhi, Synthesis and scale inhibition of modified polyaspartic acid, *Ind. Water Treat.* 28 (2008) 38–40.
- [20] L.J. Gao, N. Guo, Q.P. Mou, Z.Y. Wang, Y.S. Zhuo, H.Q. Wang, Synthesis and performance of polyaspartic acid derivatives, *Petrochem. Technol.* 32 (2003) 792–794.
- [21] Y.S. Zhao, H.M. Song, Y.M. Liu, J. Guo, Study on synthesis of poly(aspartic) acid derivatives with hydroxyl in water, *Modern Chemical Ind.* 28 (2008) 56–57.
- [22] S.K. Shukla, M.A. Quraishi, Cefotaxime sodium: A new and efficient corrosion inhibitor for mild steel in hydrochloric acid solution, *Corros. Sci.* 51 (2009) 1007–1011.
- [23] J.Y. Li, Y.B. Ao, D.F. Zeng, Study on synthesis and inhibition performance of PASP, *Appl. Chem. Ind.* 37 (2008) 770–776.
- [24] Z.H. Shen, J.S. Li, K. Xu, L.L. Ding, H.Q. Ren, The effect of synthesized hydrolyzed polymaleic anhydride (HPMA) on the crystal of calcium carbonate, *Desalination* 284 (2012) 238–244.